EurJIC
European Journal of Inorganic Chemistry

Full Papers
doi.org/10.1002/ejic.202100377

Chemistry Europe
European Chemical Societies Publishing

Anion Effect on the Formation of Zinc-Salicyaldimine Compounds in Neutral and Anionic Complex Forms: Synthesis, Characterization, ^{1}H NMR Studies, and Photophysical Properties

Meng-Jung Tsai[+],[a] Yo-Ting Su[+],[a] and Jing-Yun Wu*[a]

Reactions of $Zn(BF_4)_2$ and $ZnCl_2$ with a nitrile-functionalized salicyaldimine ligand, 3-(salicylideneimino)benzonitrile (Hsal-3-PhCN), in both 1:1 and 1:2 stoichiometry of metal-to-ligand, afforded zinc-salicyaldimine compounds $[Zn(sal\text{-}3\text{-}PhCN)_2]$ (**1**) and $[HNEt_3][Zn(sal\text{-}3\text{-}PhCN)Cl_2]$ (**2**), respectively. Compound **1** is a neutral zinc-salicyaldimine complex, where the Zn(II) center is in a distorted $\{ZnN_2O_2\}$ tetrahedral geometry, made up of two sal-3-PhCN ligands both in the N,O-chelating mode. Comparably, **2** is an ionic zinc-salicyaldimine compound, where the Zn(II) center is in a distorted $\{ZnNOCl_2\}$ tetrahedral geometry, made up of one sal-3-PhCN ligand in the N,O-chelating mode and two chloro ligands. The results indicate that neutral and anionic forms of zinc-salicyaldimine complexes would form under the domination of anion with different zinc-binding abilities. ^{1}H NMR studies indicate different degrees of decomplexation of **2** in different solvents, leading to a dynamic equilibrium between the zinc-salicyaldimine complex form and the neutral form of salicyaldimine ligand. This is achieved by proton transfer and interpreted by the hydrogen-bonding properties of the solvents. Photophysical studies reveal that Hsal-3-PhCN exhibited weak yellow fluorescence (λ_{em} = 554 nm) while **1** and **2** emitted strong blue (λ_{em} = 472 nm) and green (λ_{em} = 504 nm) fluorescence, respectively, in solid-state, and in comparison, much weaker emissions in solution phases.

Introduction

Salicyaldimines, also called salicylaldehyde Schiff bases or imine-phenol Schiff bases,[1] are half-salen-type ligands showing coordinate properties similar to that of 8-hydroxyquinoline since those ligands usually demonstrate the chelation of imine nitrogen atom and phenoxo oxygen atom to metal center,[2] i.e., a N,O-chelating systems in coordination chemistry. In addition, salicyaldimines and 8-hydroxyquinoline have similar delocalized π-systems which result in an analogy between the emission behaviors of both types of compounds.[2,3] Therefore, metal complexes of salicyaldimines have been previously studied about their structures, properties, and reactions and have important contributions to the development of catalysis,[4,5] magnetism,[6,7] luminescence,[8–10] biological activities,[11,12] molecular architectures,[13–15] and materials chemistry.

Zinc is recognized as one of the most important transition-metal ions in the human body, where it dominates multiple biological functions.[16–18] As a closed shell d^{10} transition-metal ion, zinc(II) ion lacks ligand field stabilization energy and thus forms complexes of various coordination numbers and geometries that are able to modulate the properties of coordination environments. Further, zinc(II) ion is optical-inactive showing no essential d–d electronic transitions. Therefore, fluorescence-responsive zinc complexes are encouraged to have the lowest energy excited states mainly originated from a ligand-centered charge transfer (LCT) (or intraligand charge transfer, ILCT) and/or ligand-to-ligand charge transfer (LLCT), rarely arose from ligand-to-metal charge transfer (LMCT) states involving s or p empty orbitals of the metal.[19,20]

Zinc(II) complexes of salicyaldimines are expected to exhibit not only good fluorescence properties but also fluorescence tuning both in intensity and/or in wavelength,[20,21] which are relevant to the substitution of ligands and the coordination pattern imposed by the ligands.[20,22–25] Therefore, zinc-salicyaldimine complexes have showed potential as light-emitting layers[22,26,27] and fluorescent sensors.[28,29] For example, the chiral Zn(II) complex $[Zn(HL^1)Cl_2]$ (HL^1 = 4-methyl-2,6-di[(*S*)-(+)-1-phenylethyliminomethyl] phenol), where the zinc(II) center is four-coordinated with one phenolato oxygen and one imine nitrogen from the ligand HL^1, and two chloride ligands in a distorted tetrahedral geometry, self-assembles via C–H···Cl hydrogen bonds into supramolecular left-handed helices and exhibits emission properties at room temperature.[21] The binuclear complex $[Zn_2(L^2)_2]$ (H_2L^2 = N,N′-bis(2-hydroxybenzilidene)-2,4,6-trimethylbenzene-1,3-diamine), where the zinc(II) center is coordinated by phenolato oxygen and imine nitrogen from two ligands leading to a distorted tetrahedral geometry, could act as a fluorescent probe for selective detection of Cu^{2+}/Ag^+ ions under aqueous conditions.[10]

In this paper, we report two zinc-salicyaldimine compounds **1** and **2** from the complexation reactions of a nitrile-functional-

[a] Dr. M.-J. Tsai,[+] Y.-T. Su,[+] Prof. Dr. J.-Y. Wu
Department of Applied Chemistry
National Chi Nan University,
Nantou 545, Taiwan
E-mail: jyunwu@ncnu.edu.tw
http://ibestpark.ito.tw/doac/member-detail/16_5/

[+] These authors contributed equally to this paper.

Supporting information for this article is available on the WWW under https://doi.org/10.1002/ejic.202100377

ized salicyaldimine ligand, namely 3-(salicylideneimino) benzonitrile (Hsal-3-PhCN), and zinc salts of tetrafluoroborate (BF_4^-) and chloride (Cl^-), respectively. Spectroscopic studies and solid-state structure analysis indicated that compound **1** has a neutral ML_2 type zinc-salicyaldimine structure while **2** reveals an anionic ML type zinc-salicyaldimine structure. Anions of starting metal salts were found to be responsible for forming zinc-salicyaldimine structures in the neutral ML_2 and anionic ML types. Further, ^{1}H NMR spectroscopy confirmed that ionic zinc-salicyaldimine compound **2** displayed solvent-dependent de-complexation, leading to a dynamic equilibrium between the zinc-salicyaldimine complex form and the neutral form of salicyaldimine ligand. In addition, the photoluminescent properties of Hsal-3-PhCN ligand and zinc-salicyaldimine compounds **1** and **2** were investigated.

Results and Discussion

Synthesis and Characterization of Salicyaldimine Ligand

The nitrile-functionalized salicyaldimine ligand, abbreviated as Hsal-3-PhCN, was synthesized by one-pot aldehyde-amine condensation reaction of salicylaldehyde and 3-aminobenzonitrile with a 1:1 molar ratio in methanol (CH_3OH) at room temperature, as shown in Scheme S1, with an excellent yield and high purity. ^{1}H NMR spectroscopy indicates that the azomethine proton (–*CH*=N–) signal at $\delta = 8.99$ ppm and the phenol proton signal at $\delta = 12.52$ ppm were clearly detectable in deuterated dimethylsulfoxide (DMSO-d_6) solvent (Figure S1). Mass spectroscopy exhibits an intense major peak at $m/z =$ 223.046 (Figure S2), corresponsing to the molecular ion of [Hsal-3-PhCN + H]$^+$. Furhter, the infrared spectrum shows that the most diagnostic absorption bands are the C≡N and the C=N stretching modes, occurring at 2226 and 1614 cm^{-1}, respectively (Figure S3). All of these spectroscopic observations confirm the Schiff base condensation reaction. In addition, the molecualr structure of Hsal-3-PhCN is further confirmed by single-crystal X-ray diffraction analysis, showing identical results as literature report.[30]

Synthesis and Characterization of Zinc-Salicyaldimine Compounds

The complexation reactions of $Zn(BF_4)_2$ and Hsal-3-PhCN with 1:1 or 1:2 stoichiometry of metal-to-ligand in the presence of several drops of triethylamine (NEt_3) in a tetrahydrofuran (THF) –CH_3OH solution yielded a ML_2-type zinc-salicyaldimine compound formulated as [Zn(sal-3-PhCN)$_2$] (**1**), as shown in Scheme 1. When the same reactions were carried out by using $ZnCl_2$ instead of $Zn(BF_4)_2$, a ML-type ionic zinc-salicyaldimine compound formulated as [$HNEt_3$][Zn(sal-3-PhCN)Cl_2] (**2**) was formed. The infrared spectra showed the strong $\nu_{C=N}$ stretching band occurring at 1608 cm^{-1} for **1** and 1610 cm^{-1} for **2** (Figure S3), both of which are shifted towards lower wavenumbers compared to that of the free Hsal-3-PhCN ligand (1614 cm^{-1}), indication of coordination of the azomethine nitrogen atoms with the zinc centers. Noteworthy, ^{1}H NMR spectroscopy clearly indicated that stoichiometry of metal-to-ligand has no influence while anion shows domination on the formation of ML_2 or ML type zinc-salicyaldimine compounds (Figure 1 and Figures S6–S9). The ^{1}H NMR spectra of ML_2-type zinc-salicyaldimine compound **1** in DMSO-d_6 showed a set of remarkably sharp signals, for which the phenol proton for free Hsal-3-PhCN at $\delta = 12.52$ ppm disappeared whereas the azomethine proton showed a large upfield shift from $\delta = 8.99$ ppm for free Hsal-3-PhCN to $\delta = 8.55$ ppm for **1**. On the other hand, the ^{1}H NMR spectra of ML-type ionic zinc-salicyaldimine compound **2** in DMSO-d_6 clearly demonstrated two sets of signals in the aromatic region and one set of signals in the aliphatic region (Figures S8 and S9). In the aromatic region, the two sets signals can be well-resolved to be one set of zinc-salicyaldimine complex form and one set of neutral form of Hsal-3-PhCN

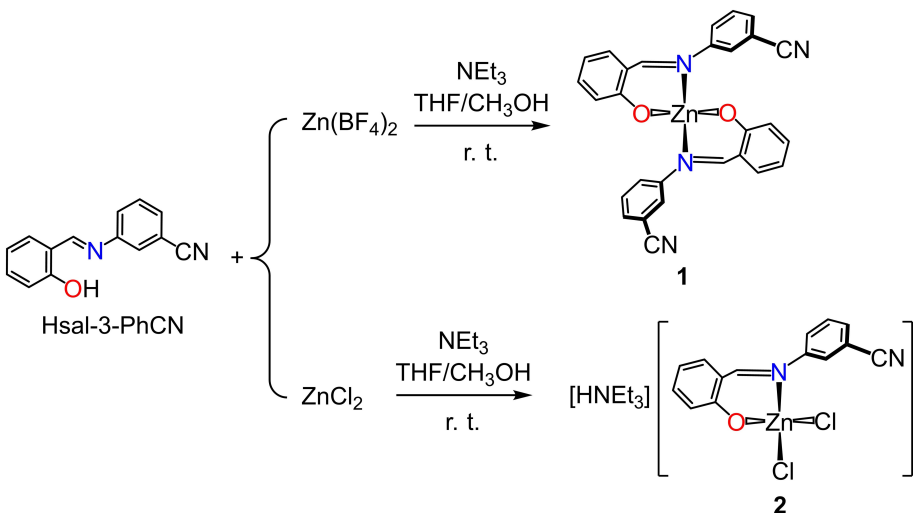

Scheme 1. Synthesis of **1** and **2**

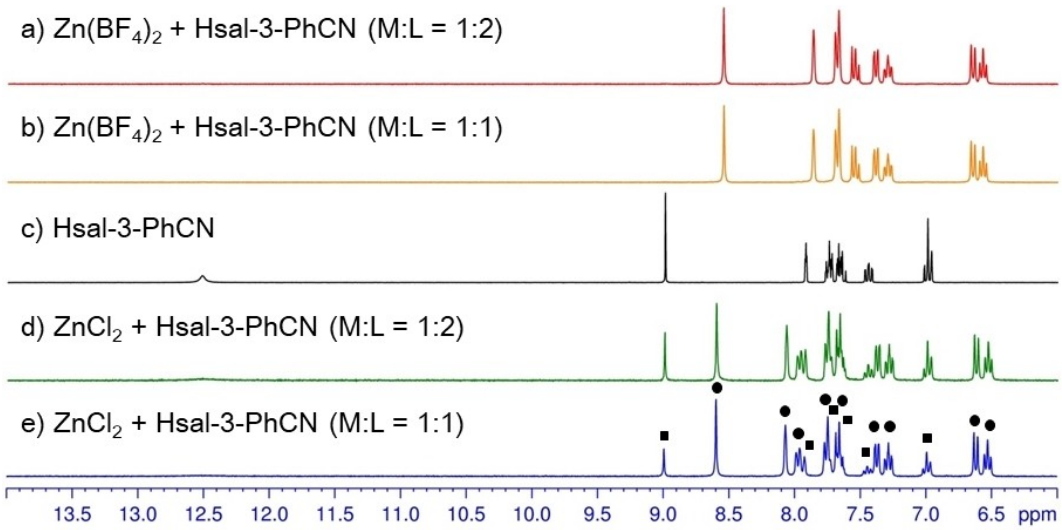

Figure 1. The aromatic region of ^{1}H NMR spectra of [Zn(sal-3-PhCN)$_2$] (**1**) obtained from the complexation of $Zn(BF_4)_2$ and Hsal-3-PhCN with a) 1:2 and b) 1:1 stoichiometry of metal-to-ligand, c) Hsal-3-PhCN, and [HNEt$_3$][Zn(sal-3-PhCN)Cl$_2$] (**2**) obtained from the complexation of $ZnCl_2$ and Hsal-3-PhCN with d) 1:2 and e) 1:1 stoichiometry of metal-to-ligand in DMSO-d_6 at room temperature. In e), soild square (■) and solid circle (●) symbols represent the two sets of signals assigning to the neutral Hsal-3-PhCN ligand and the anionic complex part, $[Zn(sal\text{-}3\text{-}PhCN)Cl_2]^-$, of **2**, respectively.

ligand (Figure 1). In the aliphatic region, one quartet resonace signal at $\delta = 2.90$ ppm and one triplet resonace signal at $\delta = 1.10$ ppm would be assigned to the methylene ($HN(CH_2CH_3)_3^+$) and methyl ($HN(CH_2CH_3)_3^+$) protons, respectively, of the triethylammonium ($HNEt_3^+$) cation of **2**. However, it is of particular note that the set of signals for the neutral form of salicyaldimine ligand always appeared in the ^{1}H NMR spectra of **2** in several independent ^{1}H NMR measurements, even dissolving the crystalline samples. The simultaneous existence of both the zinc-salicyaldimine complex form and the neutral form of salicyaldimine ligand in solution reasonably implies the presence of a dynamic equilibrium between decomplxation and recomplexation, which can be probably processed through proton transfer between the triethylammonium cations and the phenoxo groups.[23,31] Similar phenomena have also been observed for a series of ionic zinc-salicyaldimine analogues, [HNEt$_3$][Zn(salicyaldimine)Cl$_2$] (salicyaldimine = 4-(salicylideneimino)benzonitrile, 4-(5′-chlorosalicylideneimino)benzonitrile, 4-(5′-bromorosalicylideneimino)benzonitrile, and 4-(5′-methoxysalicylideneimino)benzonitrile), which showed remarkable concentration-, solvent-, and substitutent-dependent decomplxation/recomplexation equilibria in solution phases.[23]

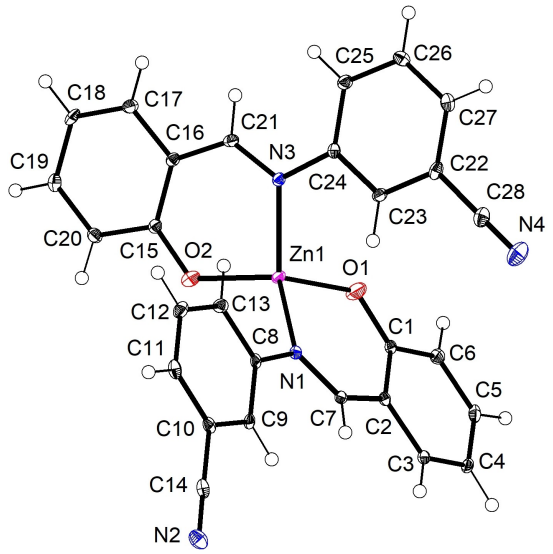

Figure 2. ORTEP plot of **1**. Displacement ellipsoids are drawn at the 30% probability level.

Crystal Structure of [Zn(sal-3-PhCN)$_2$] (1)

Single-crystal X-ray structure analysis indicated that **1** crystallized in triclinic space group $P\bar{1}$. The asymmetric unit contains one Zn(II) center and two sal-3-PhCN ligands. The Zn(II) center is coordinated by two sal-3-PhCN ligands both in the N,O-chelating mode, giving rise to a distorted tetrahedral geometry (Figure 2). The Zn–$O_{phenoxo}$ bond lengths are Zn1–O1 = 1.9195(13) Å and Zn1–O2 = 1.9125(14) Å, and the Zn–N_{imino} bond lengths are Zn1–N1 = 2.0151(17) Å and Zn1–N3 = 2.0162(17) Å (Table S1). The C=N_{imino} bond lengths are C7–N1 = 1.307(3) Å and C21–N3 = 1.308(3) Å and the C≡$N_{nitrile}$ bond lengths are C14–N2 = 1.147(3) Å and C28–N4 = 1.144(3) Å, referring to typical double bond and triple bond, respectively. Of particular note, the C=N_{imino} bond lengths are somewhat longer than that (1.277 (4) Å)[30] for free Hsal-3-PhCN ligand, as a result of Zn coordination that causes significant reduction of C=N bond order. The two chelating sal-3-PhCN ligands show the bite angles of O1–Zn1–N1 = 95.83(6)° and O2–Zn1–N3 = 96.84(6)°. The dihedral angles between the benzonitrile phenyl ring and the salicyaldimine phenyl ring of the same sal-3-PhCN ligand are 10.30 and 5.66°. Zinc-salicyaldimine analogues of

[Zn(salicyaldimine)$_2$] structure have also been observed, where salicyaldimine = salicylidene-aniline, salicylidene-p-methylaniline, salicylidene-p-methoxyaniline, salicylidene-p-cyanoaniline, salicylidene(4-dimethylamino)aniline.[22,27,32] A comparison with relevant crystallographic structural data reported in the literature on analogous tetrahedral [Zn(salicyaldimine)$_2$] complexes are provided in Table S2.

Crystal Structure of [HNEt$_3$][Zn(sal-3-PhCN)Cl$_2$] (2)

Single-crystal X-ray structure analysis indicated that **2** crystallized in monoclinic space group $P2_1/c$. The asymmetric unit consists of two distinct [Zn(sal-3-PhCN)Cl$_2$]$^-$ anions associated two distinct triethylammonium cations, [HNEt$_3$]$^+$, as counterpart. Each Zn(II) center is coordinated by one sal-3-PhCN ligand in the N,O-chelating mode and two Cl ligands, giving rise to a distorted tetrahedral geometry (Figure 3 and Figure S14). The Zn–O$_{phenoxo}$ bond lengths are Zn1–O1 = 1.9171(15) Å and Zn2–O2 = 1.9220(13) Å, the Zn–N$_{imino}$ bond lengths are Zn1–N1 = 2.0337(15) Å and Zn2–N4 = 2.0138(15) Å, and the Zn–Cl bond lengths are Zn1–Cl1 = 2.2830(5), Zn1–Cl2 = 2.2324(5), Zn2–Cl3 = 2.2419(5), and Zn2–Cl4 = 2.2698(5) Å (Table S1). The C=N$_{imino}$ bond lengths are typical double bond, where C7–N1 bond length is 1.300(2) Å and C27–N4 bond length is 1.302(2) Å, both of which are similar to those in **1** but somewhat longer than that (1.277 (4) Å)[30] in free Hsal-3-PhCN ligand due to Zn coordination induced bond order reduction. The C≡N$_{nitrile}$ bond lengths are typical triple bond, where C14–N2 bond length is 1.138(3) Å and C34–N5 bond length is 1.143(3) Å. The two chelating sal-3-PhCN ligands show the bite angles of O1–Zn1–N1 = 96.96(6)° and O2–Zn2–N4 = 97.57(6)°. The dihedral angles between the benzonitrile phenyl ring and the salicyaldimine phenyl ring of the same sal-3-PhCN ligand are 23.83 and 36.86° for the one chelating to Zn(1) and Zn(2), respectively. The [HNEt$_3$]$^+$ cation and the [Zn(sal-3-PhCN)Cl$_2$]$^{2-}$ anion attract each other through electrostatic force associated with moderate N–H···Cl hydrogen-bonding interaction between the triethylammonium proton and the chloro ligand, with the N···Cl distance of 3.199(2) Å for N3–H101···Cl1 and 3.210(2) Å for N6–H102···Cl4#1 (#1 = 1 + x, y, z) (Table S3). Of note, ML-type ionic zinc-salicyaldimine analogues, [HNEt$_3$][Zn-(salicyaldimine)Cl$_2$] (salicyaldimine = 4-(salicylideneimino) benzonitrile, 4-(5′-chlorosalicylideneimino)benzonitrile, 4-(5′-bromorosalicylideneimino)benzonitrile, and 4-(5′-methoxysalicylideneimino)benzonitrile) have been documented.[23] However, these zinc-salicyaldimine analogues showed that the hydrogen-bonding interaction is formed between the triethylammonium proton of the [HNEt$_3$]$^+$ cation and the phenoxo oxygen of the [Zn(salicyaldimine)Cl$_2$]$^-$ anion; this shows remarkable difference from that observed in **2**.

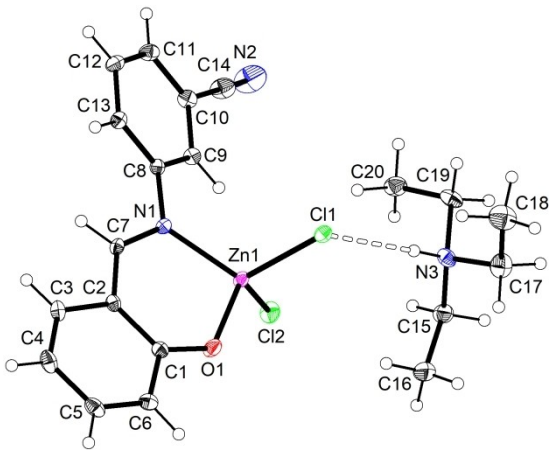

Figure 3. ORTEP plot of one of the two crystallographic distinct molecules in **2**. Displacement ellipsoids are drawn at the 30% probability level. Empty dashed line represents the N–H···Cl hydrogen bond.

^{1}H NMR Studies of 2

In order to investigate the influence of solvent on the decomplxation/recomplexation properties of **2**, the ^{1}H NMR spectra in a series of deuterated solvents including DMSO-d_6, CD_2Cl_2, acetone-d_6, CD_3CN, and CD_3OD were recorded at a concentration of approaximately 1.0×10^{-2} M (Figure 4 and Figures S9–S13). As a representative, the degree of decomplxation of **2** is influenced by used solvents, which can be addressed in terms of the dissociation ratio (R_D) parameter calculated from the equation:

$$R_D = \frac{I_{CH=N}(Hsal-3-PhCN)}{I_{CH=N}(Hsal-3-PhCN) + I_{CH=N}([Zn(sal-3-PhCN)Cl_2]^-)} \times 100$$

where $I_{CH=N}$(Hsal-3-PhCN) and $I_{CH=N}$([Zn(sal-3-PhCN)Cl$_2$]$^-$) are the relative integrated areas of the azomethine proton signal of the neutral ligand form and the complex form, respectively. Accordingly, the R_D values in these deuterated solvents are given in a trend as CD_2Cl_2 (R_D = 51.7) > DMSO-d_6 (R_D = 25.4) > acetone-d_6 (R_D = 7.4) ~ CD_3CN (R_D = 5.7) > CD_3OD (R_D = ~0), confirming the strong impact of solvent on the decomplxation of **2**.

Generally, solvent polarity, *i.e.*, the ability of the solvent to take part in strong intermolecular interactions with other like molecules, is usually to address the influence of solvent strength.[33] However, this seems not to be the domination for the decomplxation of **2** since that the given trend of polarity parameters of CH_3OH (P' = 6.6) > DMSO (P' = 6.5) > CH_3CN (P' = 6.2) > acetone (P' = 5.4) > CH_2Cl_2 (P' = 3.4) is not consistent with the R_D trend. On the other hand, it is noted that the hydrogen-bonding properties of the solvents may be responsible for the decomplxation of **2**. The greatest decomplexation occurred when dissolving **2** in CH_2Cl_2 that has no obvious H-acceptor and H-donor characteristics, followed in DMSO, acetone, and CH_3CN, that have weak to moderate H-acceptor but no H-donor characteristics, and the least decomplexation feature was observed when dissolving **2** in CH_3OH that is a good H-acceptor and H-donor solvent. This makes sense because proton transfer might be facilitated when hydrogen bonds formed directly

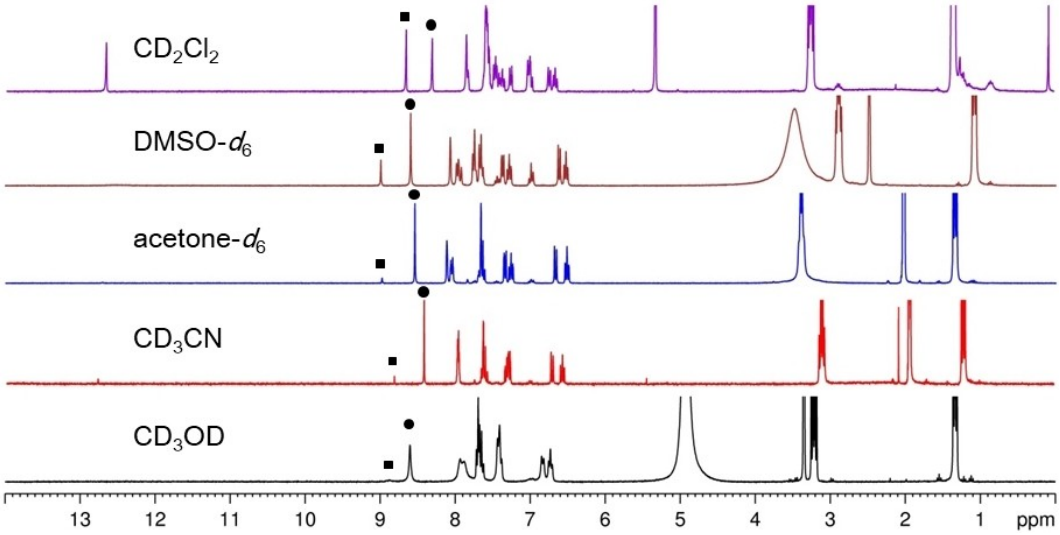

Figure 4. ^{1}H NMR spectra of $[HNEt_3][Zn(sal\text{-}3\text{-}PhCN)Cl_2]$ (**2**) in various deuterated solvents with a concentration of approaximately 1.0×10^{-2} M at room temperature. Solid square (■) and solid circle (●) symbols indicate the azomethine proton signals of the neutral ligand form of Hsal-3-PhCN and the complex form of $[Zn(sal\text{-}3\text{-}PhCN)Cl_2]^-$, respectively.

between the triethylammonium cations and the phenolato groups of the sal-3-PhCN ligand of the $[Zn(sal\text{-}3\text{-}PhCN)Cl_2]^-$ anions in CH_2Cl_2 and thus resulted in a high degree of decomplexation. Comparably, when the triethylammonium cations and the $[Zn(sal\text{-}3\text{-}PhCN)Cl_2]^-$ anions both were surrounded by H-acceptor and/or H-donor solvents such as DMSO, acetone, CH_3CN, and especially CH_3OH, proton transfer might be inhibited and thus the complex form of $[Zn(sal\text{-}3\text{-}PhCN)Cl_2]^-$ was retained.

Further, a simple assumption is that the decomplexation of **2** gives a neutral Hsal-3-PhCN ligand and a $ZnCl_2\cdot NEt_3$ species in equal equivalent as shown below:

$$[HNEt_3][Zn(sal\text{-}3\text{-}PhCN)Cl_2] \rightleftharpoons \text{Hsal-3-PhCN} + ZnCl_2\cdot NEt_3 \qquad K_{decplx}$$

The decomplxation constant (K_{decplx}) for the dynamic decomplxation/recomplexation equilibrium can be determined using the equation:

$$K_{decplx} = \frac{[Hsal-3-PhCN]\times[ZnCl_2\cdot NEt_3]}{[[HNEt_3][Zn(sal-3-PhCNL)Cl_2]]}$$

This equation can also be expressed in terms of the dissociation ratio parameter, R_D, and the initial concentration of **2**, $[[HNEt_3][Zn(sal\text{-}3\text{-}PhCN)Cl_2]]_0$, as

$$K_{decplx} = \frac{(R_D)^2}{100\times(100-R_D)} \times [[HNEt_3][Zn(sal-3-PhCN)Cl_2]]_0$$

In this study, the initial concentration of $[HNEt_3][Zn(sal\text{-}3\text{-}PhCN)Cl_2]$ is set in 1.0×10^{-2} M. As a result, the K_{decplx} values are calculated to be ~0 M in CH_3OH, 3.45×10^{-5} M in CH_3CN, 5.91×10^{-5} M in acetone, 8.65×10^{-4} M in DMSO, and 5.53×10^{-3} M in CH_2Cl_2. Similar to R_D value, the large K_{decplx} value indicates the high degree of decomplexation of **2** in solution phase. Accordingly, the degree of decomplexation of **2** in varied solvents is in the order $CH_2Cl_2 > DMSO > acetone \sim CH_3CN > CH_3OH$. Table 1 summarizes the analyses of dissociation ratios and decomplexation constants for **2** in various solvents.

Photophysical Properties

The optical absorption and fluorescence excitation spectra for Hsal-3-PhCN, **1**, and **2** were investigated in various solvents and in solid-state at room temperature (Figure 5 and Figure S15). The relvant photophysical data are provided in Table 2. The UV-Vis absorption spectra of Hsal-3-PhCN and zinc-salicyaldimine compounds **1** and **2** in solution phases including CH_2Cl_2, DMSO, acetone, CH_3CN, and CH_3OH with a concentration of 1.0×10^{-4} M exhibited no significant solvatochromism. The UV-Vis absorption spectra of Hsal-3-PhCN recorded in CH_2Cl_2, DMSO, CH_3CN, and CH_3OH all displayed two strong absorption bands at about 275 and 341 nm together with a relative weak absorption band at about 318 nm (Figure 5a). These bands can mostly be ascribed to the typical electronic transition of an aromatic ring ($\pi\rightarrow\pi^*$) and –C=N– conjugate system ($\pi\rightarrow\pi^*$ and $n\rightarrow\pi^*$) in a Schiff molecule.[10,23,25,34,35] Acetone has strong interference in 250–325 nm, hiding the high-energy absorption

Table 1. Dissociation ratios (R_D) and decomplexation constants (K_{decplx}) of zinc-salicyaldimine compound **2** in various solvents at room temperature with an initial concentration of 1.0×10^{-2} M.

	CH_3OH	CH_3CN	Acetone	DMSO	CH_2Cl_2
R_D	~0	5.7	7.4	25.4	51.7
K_{decplx} (M)	~0	3.45×10^{-5}	5.91×10^{-5}	8.65×10^{-4}	5.53×10^{-3}

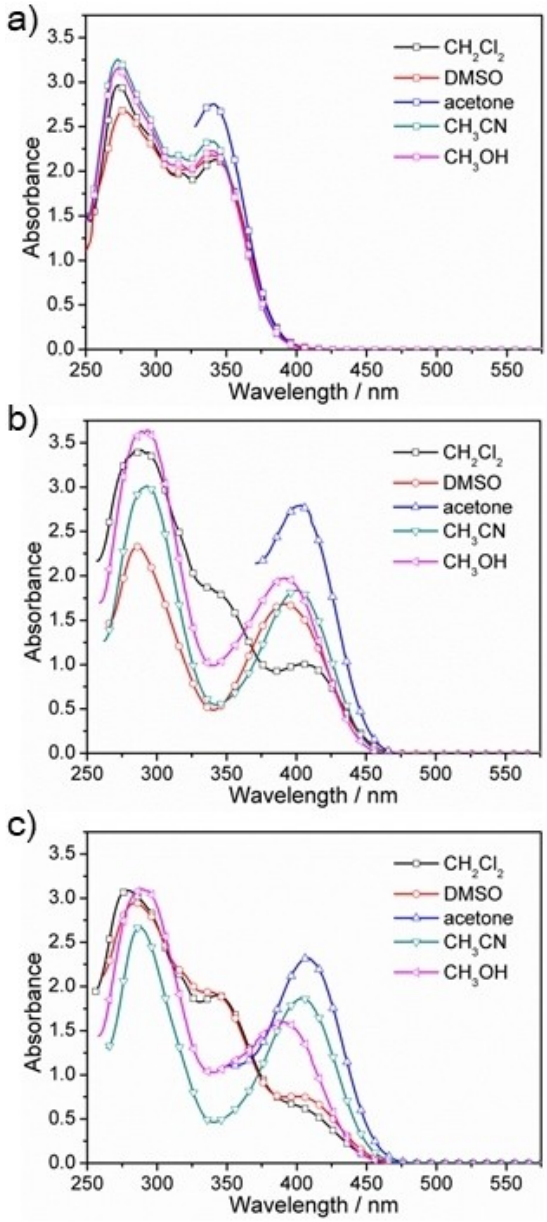

Figure 5. UV-Vis absorption spectra of a) Hsal-3-PhCN, b) **1**, and c) **2** in various solvents (1.0×10^{-4} M) at room temperature.

bands of about 275 and 318 nm and leaving only the low-energy absorption band of about 341 nm for Hsal-3-PhCN. For zinc-salicyaldimine compounds **1** and **2**, their UV-Vis absorption spectra showed an intense absorption band in the UV wavelength region of 280–293 nm and a moderately intense absorption band in the visible wavelength region of 390–407 nm (Figures 5b–5c). With reference to those for Hsal-3-PhCN, the high-energy absorption bands are originated from ILCT transitions ($\pi\rightarrow\pi^*$) whereas the low-energy absorption bands, absent in the absorption spectra of free ligand, are assigned to involve both the ligand and the metal center, probably due to the coordination of C=N to the metal, showing the d^{10}(Zn)$\rightarrow\pi^*$(azomethine) character.[35,36] Again, **1** and **2** in acetone showed only the low-energy absorption band in the visible wavelength region due to the solvent interference in the UV wavelength region. In some cases, one further ILCT transition ($n\rightarrow\pi^*$) was also observed as a shoulder band for **1** in CH_2Cl_2 (ca. 337 nm) and for **2** in CH_2Cl_2 (ca. 343 nm) and DMSO (ca. 337 nm). However, the spectra of the zinc-salicyaldimine compounds taken in in five different solvents (CH_2Cl_2, DMSO, acetone, CH_3CN, and CH_3OH) do not exhibit any significant solvatochromism. For Hsal-3-PhCN, **1**, and **2**, their solid-state excitation spectra are very similar, with two bands at around 280 and 366 nm, and a further band at 452 nm for **2** (Figure S15).

The photoluminescence spectra and quantum yields (Φ_{PL}) of Hsal-3-PhCN and zinc-salicyaldimine compounds **1** and **2** have also been investigated in solid-state and in solution phases of various solvents (Figure 6). Upon excitation, Hsal-3-PhCN exhibited weak yellow-light fluorescence centered at $\lambda_{em}=554$ nm in solid-state but silent fluorescence in solution phases (Figure 6a and Figure 6d). The quantum yields of Hsal-3-PhCN in solid-state and in various solution phases were measured to be 0.096 and 0.0004–0.001, respectively (Table 2). This property shows similarity with other salicyaldimine derivatives and can be interpreted by a photoinduced electron transfer (PET) process due to the presence of lone pair of electrons of the donor atom in the salicyaldimine ligand, thus quenching the fluorescence of the salicyaldimine compounds.[36–38] On the other hand, zinc-salicyaldimine compounds **1** and **2** emitted strong blue-light ($\lambda_{em}=472$ nm, $\Phi_{PL}=0.255$) and green-light ($\lambda_{em}=504$ nm, $\Phi_{PL}=0.385$) fluorescence, respectively, in solid-state (Figures 6b–6d), which are tentatively ascribed to ILCT emission of the compounds[31,36,39] due to that divalent zinc ion with stable d^{10} electronic configuration is redox-inert to prevent metal-based charge transfers.[40] In comparison to Hsal-3-PhCN, the fluorescence emissions for **1** and **2** are blue-shifted by 82 and 50 nm, respectively, in wavelength and enhanced by about 2.7 and 4.0 times, respectively, in quantum yield. Upon complexation, an excitate state centered on the bonded salicyaldimine ligand might be lowering in energy, resulting in a qualitative blue shift of the fluorescence emission maximum.[20,21,39] Meanwhile, complex formation with the chelation of azomethine nitrogen and phenolate oxygen atoms causes chelation enhanced fluorescence (CHEF) effect[38,41,42] and inhibits the C=N isomerization.[43–46] This significantly not only reduces the PET quenching effect but also increases structure rigidity to reduce the probability of non-radiative relaxation process by vibrational and rotational decay. As a result, the fluorescent intensity increases greatly. In solution phases, zinc-salicyaldimine compounds **1** and **2** showed weak fluorescence centered at 470–508 and 500–508 nm, respectively (Figure 6b and Figure 6c). The quantum yields of **1** and **2** in various solution phases were measured to be 0.023–0.070 and 0.022–0.098, respectively, which are much lower than that in solid-state.

Table 2. Photophysical data for Hsal-3-PhCN, **1**, and **2** in various solvents (1.0×10^{-4} M) and in solid-state at room temperature.

Compound	Medium	Absorption/excitation λ_{max} [nm] (ε [$M^{-1}cm^{-1}$])	Fluorescence λ_{max} [nm] (λ_{ex} [nm])	Φ_{PL}
Hsal-3-PhCN	CH_2Cl_2	273 (29600), 318 (19700), 342 (21200)	n.d. (340)	0.0004
	DMSO	277 (26800), 321 (20200), 340 (21800)	n.d. (340)	0.0006
	acetone	341 (27500)	n.d. (340)	0.001
	CH_3CN	273 (32500), 315 (21800), 341 (23300)	n.d. (340)	0.0005
	CH_3OH	273 (31500), 316 (20800), 341 (22200)	n.d. (340)	0.0007
	solid-state	282, 368	554 (350)	0.096
1	CH_2Cl_2	289 (34100), 337sh (18600), 404 (10000)	508 (345)	0.045
	DMSO	286 (23300), 392 (16800)	508 (390)	0.045
	acetone	403 (27900)	470 (400)	0.025
	CH_3CN	293 (30100), 400 (18300)	506 (400)	0.043
	CH_3OH	293 (36400), 392 (19700)	500 (390)	0.070
	solid-state	280, 366	472 (350)	0.255
2	CH_2Cl_2	280 (30800), 343 (19000), 399 (6600)	502 (405)	0.062
	DMSO	285 (29400), 337sh (19400), 400 (7500)	506 (405)	0.074
	acetone	407 (23200)	508 (400)	0.022
	CH_3CN	287 (26700), 404 (18600)	500 (400)	0.067
	CH_3OH	290 (31000), 390 (15900)	500 (390)	0.098
	solid-state	274, 366, 452	504 (350)	0.385

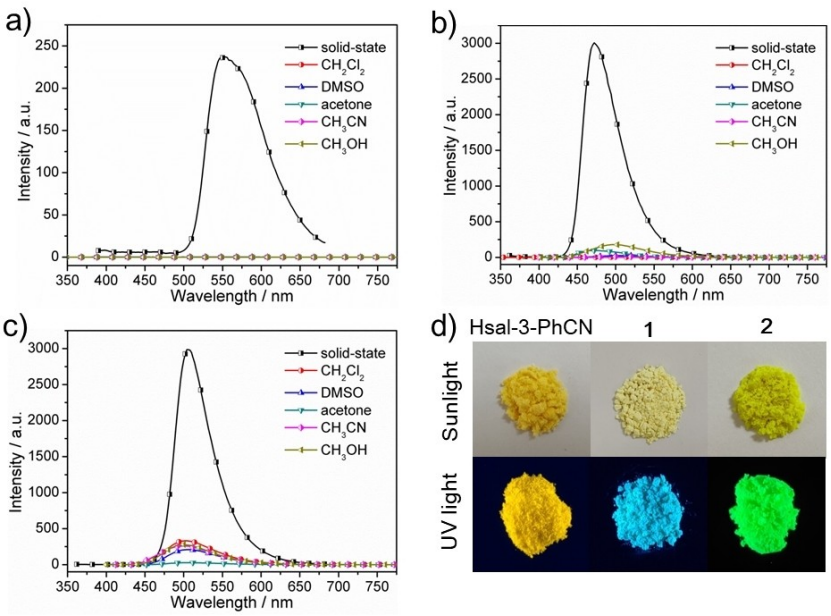

Figure 6. Photoluminescence spectra of a) Hsal-3-PhCN, b) **1**, and c) **2** in solid-state and in various solvents (1.0×10^{-4} M) at room temperature. d) Photos of solid samples of Hsal-3-PhCN, **1**, and **2** with illumination of sunlight and UV light of 365 nm.

Conclusion

Two zinc-salicyaldimine compounds have been successfully synthesized and structurally characterized. Compound [Zn(sal-3-PhCN)$_2$] (**1**) with a ML_2 complex form was obtained using $Zn(BF_4)_2$ as metal source while compound [$HNEt_3$][Zn(sal-3-PhCN)Cl_2] (**2**) with a ML complex form was prepared using $ZnCl_2$ as reagent. Varying stoichiomentry of metal-to-ligand from 1:1 to 1:2 did not affect the formation of **1** and **2**. Therefore, anion instead of metal-to-ligand molar ratio herein shows main domination on the formation of zinc-salicyaldimine compounds in ML_2 and ML complex forms. The ^{1}H NMR studies of **2** in various solvents indicate that there is equilibrium between the zinc-salicyaldimine complex form and the neutral form of salicyaldimine ligand, as a result of proton transfer induced decomplexation and recomplexation of **2** between the protonated triethylammonium cations and the phenolato groups. In particular the degree of decomplexation of **2** seems to be significantly affected by the hydrogen-bonding properties of the solvents. On the other hand, zinc-salicyaldimine compounds **1** and **2** in comparison to free salicyaldimine ligand both exhibit strong blue and green fluorescence emissions centered at $\lambda_{em}=$ 472 and $\lambda_{em}=$ 504 nm, respectively, in solid-state and in solution phases. The obtained compounds broaden an increasing family of luminescent zinc-salicyaldimine complexes.

Experimental Section

Materials and instrumentation. Chemical reagents were purchased commercially and used as received without further purification. ^{1}H NMR spectra were recorded on a Bruker AMX-300 Solution-NMR spectrometer. Chemical shifts are reported in parts per million (ppm) with reference to the residual protons of the deuterated solvent. Coupling constants are reported in hertz (Hz). Mass spectra were recorded with a Bruker Daltonics flexAnalysis matrix-assisted laser desorption/ionization time of flight (MALDI-TOF) mass spectrometer. Infrared (IR) spectra were recorded on a Perkin-Elmer RX1 Fourier transform infrared spectrometer using KBr discs in the 4000–500 cm^{-1} region. Elemental analyses were performed on an Elementar Vario EL III analytical instrument. UV-vis absorption spectra were recorded on a JASCO V-750 UV/VIS spectrophotometer. Fluorescence spectra were recorded on a Hitachi F7000 fluorescence spectrophotometer. Absolute luminescence quantum yield measurements of powders and liquid samples were conducted through the use of an integrating sphere. Melting points were measeurd on a Fargo MP-1D melting point apparatus.

Synthesis of 3-(Salicylideneimino)benzonitrile (Hsal-3-PhCN). The synthetic process for Hsal-3-PhCN was based on a previous report[29] but under a modified condition. A methanol solution (10 mL) of 3-aminobenzonitrile (0.59 g, 5.0 mmol) was added into a methanol solution (5 mL) of salicylaldehyde (0.52 mL, 5.0 mmol) under nitrogen atmosphere. The mixture was allowed to stir for 4 h at room temperature, and then the solvent was removed under reduced pressure. The resultant crush products were washed with methanol to give pure Hsal-3-PhCN as pale-yellow powders. Yield 48% (0.53 g, 2.4 mmol). ^{1}H NMR (300 MHz, DMSO-d_6, ppm): δ 12.52 (br, s, 1H), 8.99 (s, 1H), 7.93 (s, 1H), 7.92–7.72 (m, 2H), 7.69–7.61 (m, 2H), 7.44 (td, J = 8.1, 1.8 Hz, 1H), 7.00 (d, J = 7.5 Hz, 1H), 6.98 (d, J = 8.4 Hz, 1H). MS (MALDI-TOF$^+$): *m/z* 223.046 $[M+H]^+$. IR (KBr pellet, cm^{-1}): 2226 ($\nu_{C\equiv N}$), 1614 ($\nu_{C=N}$). Anal. calcd for $C_{14}H_{10}N_2O$: C, 75.66; H, 4.54; N, 12.60%. Found: C, 75.64; H, 4.50; N, 12.65%. Melting point: 114–115 °C.

*Synthesis of [Zn(sal-3-PhCN)$_2$] (**1**).* A methanol solution (12 mL) of $Zn(BF_4)_2 \cdot xH_2O$ (239.0 mg, 1.0 mmol) was added into a THF solution (10 mL) of Hsal-3-PhCN (444.0 mg, 2.0 mmol) under nitrogen atmosphere. The mixture was allowed to stir for 10 min, and then NEt_3 (99%, 18 drops, pH = 8–9) was added. The resultant solution was allowed to stir at room temperature overnight. The solvent was removed under reduced pressure and then washed with methanol. The resulting bright yellow precipitates were filtered. Yield 67% (340.0 mg, 0.67 mmol). ^{1}H NMR (300 MHz, DMSO-d_6, δ): 8.55 (s, 2H), 7.86 (s, 2H), 7.68 (d, J = 6.9 Hz, 4H), 7.54 (t, J = 7.8 Hz, 2H), 7.39 (dd, J = 7.8, 1.5 Hz, 2H), 7.30 (t, J = 7.5 Hz, 2H), 6.65 (d, J = 8.4 Hz, 2H), 6.57 (t, J = 7.2 H, 2H). MS (MALDI-TOF$^+$): *m/z* 507.150 $[M]^+$. IR (KBr pellet, cm^{-1}): 2230 ($\nu_{C\equiv N}$), 1608 ($\nu_{C=N}$). Anal. Calcd for $C_{28}H_{18}N_4O_2Zn$: C, 66.22; H, 3.57; N, 11.03%. Found: C, 65.27; H, 3.54; N, 10.81%. Melting point: 224–226 °C. Yellow plate-shaped single crystals suitable for X-ray diffraction were obtained by quietly staying the dichloromethane (CH_2Cl_2) solution of [Zn(sal-3-PhCN)$_2$] (**1**) at room temperature for one week.

*Synthesis of [HNEt$_3$][Zn(sal-3-PhCN)Cl$_2$] (**2**).* A methanol solution (7 mL) of $ZnCl_2$ (136.3 mg, 1.0 mmol) was added into a THF solution (7 mL) of Hsal-3-PhCN (222.0 mg, 1.0 mmol) under nitrogen atmosphere. The mixture was allowed to stir for 10 min, and then NEt_3 (99%, 16 drops, pH = 8–9) was added. The resultant solution was allowed to stir at room temperature overnight. The solvent was removed under reduced pressure and then ethyl ether was added. The resulting bright yellow precipitates were filtered. Yield 46% (210.0 mg, 0.46 mmol). ^{1}H NMR (300 MHz, DMSO-d_6, ppm): δ 8.60 (s, 1H), 8.07 (s, 1H), 7.97 (d, J = 7.8 Hz, 1H), 7.76 (d, J = 7.5 Hz, 1H), 7.67 (d, J = 8.1 Hz, 1H), 7.37 (dd, J = 7.8, 1.2 Hz, 1H), 7.29 (td, J = 7.8, 1.8 Hz, 1H), 6.62 (d, J = 8.7 Hz, 1H), 6.53 (t, J = 7.2 Hz, 1H), 2.90 (q, J = 7.2 Hz, 6H), 1.09 (t, J = 7.2 Hz, 9H). MS (MALDI-TOF$^+$): *m/z* 457.223 $[M]^+$ (459.73). IR (KBr pellet, cm^{-1}): 2230 ($\nu_{C\equiv N}$), 1610 ($\nu_{C=N}$). Anal. calcd for $C_{20}H_{25}Cl_2N_3OZn$: C, 52.25; H, 5.48; N, 9.14%. Found: C, 51.94; H, 5.35; N, 9.26%. Melting point: 189–191 °C. Yellow prismatic single crystals suitable for X-ray diffraction were obtained after one week by slow diffusion of ether into the methanol solution of [HNEt$_3$][Zn(sal-3-PhCN)Cl$_2$] (**2**) at room temperature.

Single-crystal structure determination. Single-crystal X-ray diffraction data collections were performed by using a Bruker Smart CCD diffractometer for **1** and a Bruker D8 Venture diffractometer for **2**. The radiation used was graphite monochromated Mo Kα radiation (λ = 0.71073 Å). Starting models for structure refinement were found using direct methods (SHELXS-97[47]) and refined against F^2 by the full-matrix least-squares technique, using the SHELXL-2014/7,[48] incorporated in WINGX-v2014.1 crystallographic collective package.[49] Non-hydrogen atoms were found from the different Fourier maps and refined with anisotropic displacement parameters. Hydrogen atoms were placed in calculated positions with isotropic displacement parameters. Experimental details for X-ray data collection and the refinements are summarized in Table 3.

Deposition Numbers 2080342 (**1**) and 2080343 (**2**) contain the supplementary crystallographic data for this paper. These data are provided free of charge by the joint Cambridge Crystallographic Data Centre and Fachinformationszentrum Karlsruhe Access Structures service www.ccdc.cam.ac.uk/structures.

Acknowledgements

We gratefully acknowledge the National Chi Nan University and the Ministry of Science and Technology of Taiwan (NSC 98-2113-M-260-004-MY2 and MOST 108-2113-M-260-002-) for the financial

Table 3. Crystallographic data for zinc-salicyaldimine compounds **1** and **2**.

	1	**2**
Empirical formula	$C_{28}H_{18}N_4O_2Zn$	$C_{20}H_{25}Cl_2N_3OZn$
M_w	507.83	459.70
Crystal system	Triclinic	Monoclinic
Space group	$P\bar{1}$	$P2_1/c$
a [Å]	8.5050(3)	13.3207(7)
b [Å]	11.0636(4)	24.6763(13)
c [Å]	12.5338(5)	14.2982(9)
α [°]	74.1250(10)	90
β [°]	78.2890(10)	113.289(2)
γ [°]	88.0510(10)	90
V [Å^3]	1110.50(7)	4317.0(4)
Z	2	8
T [K]	296(2)	150(2)
λ [Å]	0.71073	0.71073
D_{calc} [g cm^{-3}]	1.519	1.415
F_{000}	520	1904
μ [mm^{-1}]	1.141	1.400
θ_{min}, θ_{max} [°]	1.725, 25.042	2.421, 27.894
Refl. collected	14135	71401
Unique refl. (R_{int})	3850 (0.0316)	10273 (0.0521)
Obs. refl. [$I > 2\sigma(I)$]	3365	9072
Parameters	316	493
R_1,[a] wR_2[b] [$I > 2\sigma(I)$]	0.0275, 0.0578	0.0292, 0.0873
R_1,[a] wR_2[b] [all data]	0.0348, 0.0603	0.0376, 0.1028
GOF on F^2	1.048	1.161
Max., min. $\Delta\rho$ [e Å^{-3}]	0.319, −0.266	1.474, −0.952

[a] $R_1 = \sum ||F_o| - |F_c|| / \sum |F_o|$. [b] $wR_2 = \{\sum [w(F_o^2 - F_c^2)^2] / \sum [w(F_o^2)^2]\}^{1/2}$.

support. The authors thank the Instrument Center at National Chung Hsing University for providing valuable assistance on Elemental Analysis and Single Crystal X-Ray Diffractometer. The authors also acknowledge MOST for research support (MOST110-2731-M-005-001, XRD001300, EA000100).

Conflict of Interest

The authors declare no conflict of interest.

Keywords: Anion effect · Fluorescence · Salicyaldimine · Zinc

[1] X.-X. Zhou, Y.-P. Cai, S.-Z. Zhu, Q.-G. Zhan, M.-S. Liu, Z.-Y. Zhou, L. Chen, *Cryst. Growth Des.* **2008**, *8*, 2076–2079.
[2] T. Yu, W. Su, W. Li, Z. Hong, R. Hua, M. Li, B. Chu, B. Li, Z. Zhang, Z. Z. Hu, *Inorg. Chim. Acta* **2006**, *359*, 2246–2251.
[3] Y. Z. Shen, H. W. Gu, Y. Pan, G. Dong, T. Wu, X. P. Jin, X. Y. Huang, H. W. Hu, *J. Organomet. Chem.* **2000**, *605*, 234–238.
[4] G. A. Morris, H. Zhou, C. L. Stern, S. B. T. Nguyen, *Inorg. Chem.* **2001**, *40*, 3222–3227.
[5] S. Bhunora, J. Mugo, A. Bhaw-Luximon, S. Mapolie, J. Van Wyk, J. Darkwa, E. Nordlander, *Appl. Organomet. Chem.* **2011**, *25*, 133–145.
[6] S. Naiya, H. S. Wang, M. G. Drew, Y. Song, A. Ghosh, *Dalton Trans.* **2011**, *40*, 2744–2756.
[7] P. Mukherjee, M. G. Drew, C. J. Gomez-Garcia, A. Ghosh, *Inorg. Chem.* **2009**, *48*, 5848–5860.
[8] M. Shellaiah, Y.-H. Wu, A. Singh, M. V. R. Raju, H.-C. Lin, *J. Mater. Chem. A* **2013**, *1*, 1310–1318.
[9] K. B. Kim, H. Kim, E. J. Song, S. Kim, I. Noh, C. Kim, *Dalton Trans.* **2013**, *42*, 16569–16577.
[10] R. Pandey, P. Kumar, A. K. Singh, M. Shahid, P.-z. Li, S. K. Singh, Q. Xu, A. Misra, D. S. Pandey, *Inorg. Chem.* **2011**, *50*, 3189–3197.
[11] W. A. Zoubi, S. G. Mohamed, A. A. S. Al-Hamdani, A. P. Mahendradhany, Y. G. Ko, *RSC Adv.* **2018**, *8*, 23294–23318.
[12] C. P. Matos, Y. Addis, P. Nunes, S. Barroso, I. Alho, M. Martins, A. P. A. Matos, F. Marques, I. Cavaco, J. C. Pessoa, I. Correia, *J. Inorg. Biochem.* **2019**, *198*, 110727.
[13] C. J. Whiteoak, G. Salassa, A. W. Kleij, *Chem. Soc. Rev.* **2012**, *41*, 622–631.
[14] J.-Y. Wu, C.-Y. Chang, C.-J. Tsai, J.-J. Lee, *Inorg. Chem.* **2015**, *54*, 10918–10924.
[15] Y.-J. Tseng, J.-Y. Wu, *Inorg. Chim. Acta* **2017**, *455*, 241–246.
[16] C. J. Frederickson, J.-Y. Koh, A. I. Bush, *Nat. Rev. Neurosci.* **2005**, *6*, 449–462.
[17] P. J. Jiang, Z. J. Guo, *Coord. Chem. Rev.* **2004**, *248*, 205–229.
[18] N. C. Lim, H. C. Freake, C. Bruckner, *Chem. Eur. J.* **2004**, *11*, 38–49.
[19] A. Barbieri, G. Accorsi, N. Armaroli, *Chem. Commun.* **2008**, 2185–2193.
[20] R. Diana, B. Panunzi, *Molecules* **2020**, *25*, 4984.
[21] M. Prabhakar, P. S. Zacharias, S. K. Das, *Inorg. Chem.* **2005**, *44*, 2585–2587.
[22] L. Chen, J. Qiao, J. Xie, L. Duan, D. Zhang, L. Wang, Y. Qiu, *Inorg. Chim. Acta* **2009**, *362*, 2327–2333.
[23] H.-W. Chiang, Y.-T. Su, J.-Y. Wu, *Dalton Trans.* **2013**, *42*, 15169–15182.
[24] K.-L. Kuo, C.-C. Huang, Y.-C. Lin, *Dalton Trans.* **2008**, 3889–3898.
[25] S. Di Bella, I. Fragalà, I. Ledoux, M. A. Diaz-Garcia, T. J. Marks, *J. Am. Chem. Soc.* **1997**, *119*, 9550–9557.
[26] Y. Hamada, T. Sano, M. Fujita, T. Fujii, Y. Nishio, K. Shibata, *Jpn. J. Appl. Phys.* **1993**, *32*, L511–L513.
[27] J. Xie, J. Qiao, L. Wang, J. Xie, Y. Qiu, *Inorg. Chim. Acta* **2005**, *358*, 4451–4458.
[28] L. De La Durantaye, T. McCormick, X. Y. Liu, S. Wang, *Dalton Trans.* **2006**, *48*, 5675–5682.
[29] M. Maiti, S. Thakurta, D. Sadhukhan, G. Pilet, G. M. Rosair, A. Nonat, L. J. Charbonnière, S. Mitra, *Polyhedron* **2013**, *65*, 6–15.
[30] H.-J. Xu, X.-X. Gong, H. Wang, *Acta Crystallogr. Sect. E* **2008**, *64*, o638.
[31] L. Ma, L. Lu, M. Zhu, Q. Wang, Y. Li, S. Xing, X. Fu, Z. Gao, Y. Dong, *Dalton Trans.* **2011**, *40*, 6532–6540.
[32] M. D. Jones, M. G. Davidson, C. G. Keir, L. M. Hughes, M. F. Nahon, D. C. Apperley, *Eur. J. Inorg. Chem.* **2009**, 635–642.
[33] L. R. Snyder, *J. Chromatogr.* **1974**, *92*, 223–230.
[34] L. Gao, Y. Wang, J. Wang, L. Huang, L. Shi, X. Fan, Z. Zou, T. Yu, M. Zhu, Z. Li, *Inorg. Chem.* **2006**, *45*, 6844–6850.
[35] S.-N. Li, Q.-G. Zhai, M.-C. Hu, Y.-C. Jiang, *Inorg. Chim. Acta* **2009**, *362*, 2217–2221.
[36] D. Das, B. G. Chand, K. K. Sarker, J. Dinda, C. Sinha, *Polyhedron* **2006**, *25*, 2333–2340.
[37] S. Basak, S. Sen, C. Marschner, J. Baumgartner, S. R. Batten, D. R. Turner, S. Mitra, *Polyhedron* **2008**, *27*, 1193–1200.
[38] N. J. Williams, W. Gan, J. H. Reibenspies, R. D. Hancock, *Inorg. Chem.* **2009**, *48*, 1407–1415.
[39] S. Shit, M. Nandy, D. Saha, L. Zhang, W. Schmitt, C. Rizzoli, T. N. G. Row, *J. Coord. Chem.* **2016**, *69*, 2403–2414.
[40] M. Jayendran, P. M. S. Begum, M. R. P. Kurup, *J. Mol. Struct.* **2020**, *1206*, 127682.
[41] T.-H. Ma, M. Dong, Y.-M. Dong, Y.-W. Wang, Y. Peng, *Chem. Eur. J.* **2010**, *16*, 10313–10318.
[42] L. Xue, Q. Liu, H. Jiang, *Org. Lett.* **2009**, *11*, 3454–3457.
[43] D. Ray, P. K. Bharadwaj, *Inorg. Chem.* **2008**, *47*, 2252–2254.
[44] J.-R. Sheng, F. Feng, Y. Qiang, F.-G. Liang, L. Sen, F.-H. Wei, *Anal. Lett.* **2008**, *41*, 2203–2213.
[45] J.-S. Wu, W.-M. Liu, X.-Q. Zhuang, F. Wang, P.-F. Wang, S.-L. Tao, X.-H. Zhang, S.-K. Wu, S.-T. Lee, *Org. Lett.* **2007**, *9*, 33–36.
[46] Y. W. Choi, G. J. Park, Y. J. Na, H. Y. Jo, S. A. Lee, G. R. You, C. Kim, *Sens. Actuators B* **2014**, *194*, 343–352.
[47] G. M. Sheldrick, *Acta Crystallogr. Sect. A* **2008**, *64*, 112–122.
[48] G. M. Sheldrick, *Acta Crystallogr. Sect. C* **2015**, *71*, 3–8.
[49] L. J. Farrugia, *J. Appl. Crystallogr.* **2012**, *45*, 849–854.

Manuscript received: May 4, 2021
Revised manuscript received: July 9, 2021
Accepted manuscript online: July 13, 2021

FULL PAPERS

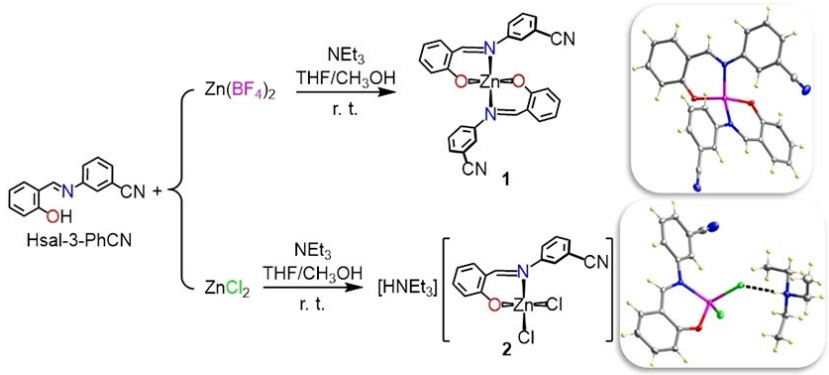

*Dr. M.-J. Tsai, Y.-T. Su, Prof. Dr. J.-Y. Wu**

Anion Effect: Anion shows remarkable domination on the formation of neutral and ionic zinc-salicyaldimine compounds, of which the ionic one exhibits solvent-dependent equilibria of decomplxation and recomplexation.